buildings

MDPI

Article

Study on the Relationship between Early Shrinkage Cracking and Mechanical Properties of Nano-Clay Cement Mortar Based on Fractal Theory

Shiyi Zhang [1,*], Zhisheng Fang [1], Wenjie Qi [1], Yingfang Fan [2,*] and Surendra P. Shah [3,4]

[1] School of Civil Engineering and Architecture, Shandong University of Technology, Zibo 255000, China
[2] Institute of Road and Bridge Engineering, Dalian Maritime University, Dalian 116026, China
[3] Department of Civil and Environmental Engineering, Northwestern University, Evanston, IL 60208, USA
[4] Department of Civil Engineering, University of Texas at Arlington, Arlington, TX 76010, USA
* Correspondence: zhangsy986@sdut.edu.cn (S.Z.); fanyf@dlmu.edu.cn (Y.F.)

Abstract: In order to study the influence of nano-clay on the crack resistance of cement-based materials, two kinds of nano-metakaolin (NMK) and two kinds of nano-attapulgite clay (NMA) were considered. The early cracking process and mechanical properties of nano-clay cement mortar (NCM) was studied by using a plate knife-edge constraint test. Based on fractal theory, the distribution characteristics of NCM surface cracks were revealed, and the calculation method forNCM maximum crack width was given. The results show that the cracking time of the NMK-3 specimen is 2 and 6 h later than that of NMK-1 and NMA-2, respectively; the smaller the particle size of nano-clay, the earlier the cracking time of the specimen. However, nano-clay effectively inhibited the expansion of mortar cracks, and the cracks on the surface of NCM were thin and sparse. At 28 days, the maximum crack width of NMK-3 was 46.7% and 33.3% lower than that of NMK-1 and NMA-2, respectively. NMK hadthe best improvement effect on the mechanical properties cement mortar. The smaller the particle size, the more pronounced the improvement effect. The flexural strength ratio and compressive strength ratio at 7 and 28 d are 76.7%, 67.4%, and 61.2%, respectively. The distribution of surface cracks on NCM has fractal characteristics, and the fractal dimension of surface cracks is smaller than that of ordinary cement mortar. The larger the particle size of nano-clay, the smaller the fractal dimension of cracks. The quantitative relationship between fracture fractal dimension and NCM elastic modulus and shrinkage tensile stress is established.

Keywords: nano-clay; cement mortar; shrinkage; cracks; fractal dimension

check for updates

Citation: Zhang, S.; Fang, Z.; Qi, W.; Fan, Y.; Shah, S.P. Study on the Relationship between Early Shrinkage Cracking and Mechanical Properties of Nano-Clay Cement Mortar Based on Fractal Theory. *Buildings* **2023**, *13*, 123. https://doi.org/10.3390/buildings13010123

Academic Editors: Jorge de Brito and Syed Minhaj Saleem Kazmi

Received: 21 October 2022
Revised: 14 December 2022
Accepted: 29 December 2022
Published: 3 January 2023

Copyright: © 2023 by the authors. Licensee MDPI, Basel, Switzerland. This article is an open access article distributed under the terms and conditions of the Creative Commons Attribution (CC BY) license (https://creativecommons.org/licenses/by/4.0/).

1. Introduction

At present, nano-materials are widely used in the repair and reinforcement of concrete structures undercracking damage. Nano-SiO_2 as the repair material has been successfully applied in the reinforcement of water conservancy projects, such as the Three Gorges Dam, the Middle Route of South-to-North Water Diversion Project, and Shangjiahe Reservoir [1,2]. In recent years, many scholars have carried out a large number of experimentstostudythe effect of nano-materials on the crack resistance of cement-based materials. The results have shown that the incorporation of nano-SiO_2, nano-$CaCO_3$, carbon nano-tubes, nano-TiO_2, etc., can improve the crack resistance of cement-based materials [3–7], but nano-silica, carbon nano-tubes, and other nano-materials are difficult to prepare and expensive, and it is difficult to promote their application [2]. Nano-clays such as nano-metakaolinand nano-attapulgite claynot only have the advantages notedabove [5–11], but also have abundant reserves and low prices. They can also promote hydration reaction, improve the cohesion of cement slurryand the internal particle characteristics of cement mortar, and make its microstructure denser. Zhang et al. [12,13] found that NMK particles can fill the pores between fibers and matrix micro-cracks and reduce the occurrence of cracks.

Kawashima et al. [14] believed that NMA can reduce the number of shrinkage cracks in cement-stabilized macadam bases. In summary, the filling effect of nano-clay reduces the porosity of cement-based materials, thereby reducing the occurrence of cracks [15,16]. However, there are few reports concerningnano-clay preventing the cracking of cement-based materials and the overalllifecycle cracking process of nano-clay cement-based materials.

Fractal geometry provides a powerful tool for describing irregular and segmented graphics other than Euclidean geometry. Fractal theory has been widely used in civil engineering. Many scholars use fractal geometry to study the fracture surfacecharacteristics of the concrete [17–19]. In the aspect of concrete material properties, Bishnoi et al. [17] carried out uniaxial tensile tests on concrete specimens and analyzed the fracture surface by fractal dimension, which showed that the roughness of the fracture surface and the stateof the crack were closely related to the heterogeneity of concrete. Zhu et al. [20] analyzed the characteristics of the fracture surface of concrete under dynamic loading by digital imagingand laser scanning technology and concluded that the higher the fractal dimension, the greater the fracture energy required at the interface. Maciej et al. [21] appliedfractal theory to study the fracture behavior of plain concrete andfiber-reinforced concrete under variouswater–cement ratios. The fracture energy was characterized by the pseudo-fractal dimension, and the fracture resistance of fiber-reinforced concrete was verified. Guo et al. [22] studied the influence ofvarious mix proportions on the fracture surface of the concrete. The results show that the fractal dimension of concrete fracture surfaces varieswith different mix proportions. Sina et al. [23] used acoustic emission technology to predict damage evolution and failure of concrete structures based on the fractal theory and multi-scale analysis. At present, research on concrete cracks under corrosive conditions is mostly focused on chloride corrosion, and concrete in actual structures is also corroded by sulfates such as acid rain. In practical engineering, damaged components are reinforced, such as CFRP and nano-materials-reinforced concrete components. The reinforced components remain affected by the corrosive environment, and the damage and destruction appear and develop again [24,25]. Thus, for better quantitative understanding of crack information in concrete members so that the safety status could be connected, fractal theory provides a promising solution. However, how efficiently and accurately fractal information can be used to indicate structural damage and performdamage assessment or classification in a generalized way remains to be studied [25].

Nano-clay has been found to be effective in facilitating casting in a numberof different applications; these case studies utilize formwork casting and slipform paving, and facilitate new ones, e.g., extrusion and 3Dconcrete printing. Although NCs have been used and studied in concretes incorporating different admixtures, e.g., SCC and SFCC, detailed studies on NC–admixture interaction are still scarce, and further investigation couldlead to improved compatibility [14]. In this study, the initial shrinkage behavior and strength performance of cement composites were evaluated through the application of nano-materials.In this study, two kinds of nano-clay materials were selected, and the development process of shrinkage cracking of nano-clay cement mortar under constraint conditions was analyzed by using the plate knife-edge constraint test method. The flexural, compressive, and tensile strengthswereevaluated by measuring the strength after various curing days. Based on the fractal theory, the surface crack distribution characteristics of the plate specimen were analyzed, and the shrinkage tensile stress and surface cracks of nano-clay cement mortar were calculated theoretically. The relationship between the fractal dimension of the surface cracks of the specimen and the elastic modulus and the shrinkage tensile stress was evaluated.

2. Experimental Study

2.1. Raw Materials

For dispersion testing, tap water and two types of nano-clay,NMA (NMA-1, NMA-2) and NMK (NMK-1, NMK-2, NMK-3, NMK-4, NMK-5), were used. Similar materials have the same chemical composition, but different particle sizes; for the chemical compositions

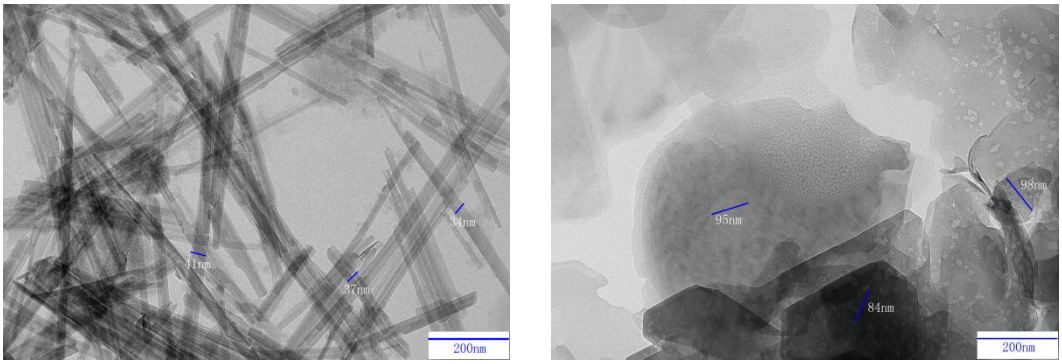
of NMA and NMK, see Table 1. The physical properties of each sample are shown in Table 2. The XRD patterns of NMA and NMK are shown in Figure 1. There are mullite crystals($3Al_2O_3 \bullet 2SiO_2$) inside the NMA, and its diffraction peak intensity is significantly higher than the dispersion peak; the crystal form is stable, and the pozzolanic activity is slightly lower. The intensity is lower than the dispersion peak, the crystal form is unstable, and it shows potential pozzolanic activity. The cement used in the test is Dalian xiao ye tian PO•42.5R ordinary Portland cement.

Table 1. Chemical composition of nano-clay (mass fraction, %).

Chemical Composition	SiO_2	CaO	Al_2O_3	Fe_2O_3	MgO	K_2O	Na_2O	Lol
NMK	47.8	0.3	41.8	0.3	0.1	0.6	0.1	9.0
NMA	50.4–61.3	1.8–2.5	9.4–9.5	4.0–5.0	9.3–10.5	0.2–0.6	0.5–1.0	11.9–13.5

Table 2. Physical performance index.

Nano-Clay Numbering	AttapulgiteClays		Nano-Metakaolin				
	NMA-1	NMA-2	NMK-1	NMK-2	NMK-3	NMK-4	NMK-5
Lamellar diameter/nm	20–100	20–100	300–500	2500	1000	300–500	100
Slice thickness/nm	-	18–25	20–50	-	-	-	80



(**a**) (**b**)

Figure 1. XRD spectra of nano-clay: (**a**) NMA; (**b**) NMK.

2.2. Preparation of Specimen

Nano-clay was dispersed in water using the ultrasonic method. The content of nano-clay was 3% of the mass of dispersed water, and the dispersion times were 5, 10, and 15 min. The test vessel was a 17 mm × 17 mm × 150 mm square tube made of quartz glass with 63 samples.

Previous studies have shown that the cracking performance of cement-based materials is improved when the nano-material content is 3% [25–27]. Therefore, the nano-clay content of cracking performance specimens is 3%. Four nano-clays, NMA-1, NMA-2, NMK-1, and NMK-3, were chosen. Using the method of manual stirring, the dry materials were first mixed evenly and then added to the nano-clay suspension by ultrasonic dispersion for 15 min, mixing evenly. The mixing protocol for cement mortar is listed in Table 3. The plated-blade constraint specimen size was 800 mm × 600 mm × 100 mm, with a total of five groups, three specimens in each group. Similarly, five groups of NCM specimens of 40 mm × 40 mm × 160 mm size, with three specimens in each group, were created. The NCM mix ratio is shown in Table 4.

Table 3. Mix protocol for cement mortar.

Time	Procedure
0:00	Disperse the clay in water
15:00	Add dry cement ingredients, mixing on low speed
17:15	Add sand in 30 s, mixing on low speed
20:00	Stop mixing, scrap edges of mixer
21:00	Mix on high speed
26:00	End of mixing

Table 4. Mix proportion of cement mortar.

Specimen Number	Cement/g	Sand/g	Water/g	NMK-1/g	NMA-1/g	NMK-3/g	NMA-2/g
MC0	4500	6750	2250	-	-	-	-
MC1	4365	6750	2250	135	-	-	-
MC2	4365	6750	2250	-	135	-	-
MC3	4365	6750	2250	-	-	135	-
MC4	4365	6750	2250	-	-	-	135

2.3. Test Methods and Processes

2.3.1. Plate Constraint Experiment

According to the Standard for Long-Term Performance and Durability of Ordinary Concrete (GB/T50082-2009), the cracking performance of NCM was tested based on the flat-blade constraint method, and the HC-CK102 crack-width measuring instrument (measurement accuracy was 0.01 mm) was used. The crack width and length of the specimens were measured after 3, 5, 7, 14, and 28 days of curing, The knife-edge restraint experiment and crack measurement are shown in Figure 2. This method can improve the cracking sensitivity and effectiveness of cement-based materials. Quantitatively comparing the cracking performance of cement-based materials improves the accuracy and repeatability of the results. According to the Guide to Durability Design and Construction of Concrete Structures (CCES 01-2004), the evaluation index of the surface cracking performance of NCM specimens is calculated using the following variables: the average cracking area of each crack a, the number of cracks per unit area b, the crack area c on the unit area, and the crack reduction coefficient n.

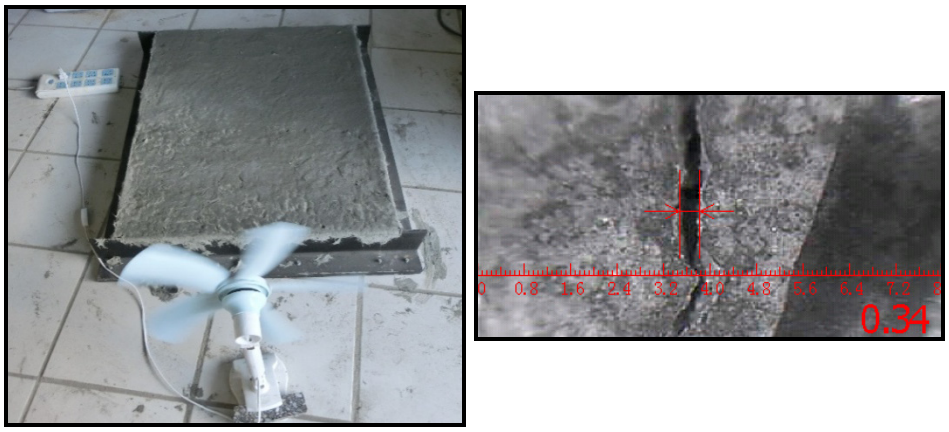


Figure 2. Flatknife-edge restraint experiment and crack test.

The average crack area $a$for each crack is calculated according to Formula (1):

$$a = \frac{1}{2N}\sum_{i=1}^{N}(W_i \times L_i) \quad (1)$$

The number of cracks per unit area b is calculated according to Formula (2):

$$b = \frac{N}{A} \tag{2}$$

The cracking area per unit area c is calculated according to Formula (3):

$$c = a \bullet b \tag{3}$$

In Formulas (1)–(3), W_i is the maximum crack width, (mm); L_i is the length of the crack, (mm); N is the number of longitudinal cracks; and A is the plate area (m^2).

2.3.2. Microstructure Analysis

A Supra 55 Sapphire field emission scanning electron microscope (SEM) was used to observe and analyze the microscopic morphological characteristics of the samples at different ages. When preparing the sample, the piece wascured to the test age and broken, and the block of about 1 cm × 1 cm × 1 cm wastaken and placed in anhydrous ethanol for 48 h to stop hydration. The test section of the sample is not subjected to any treatment.

3. Results and Discussion

3.1. Cracking and Mechanical Properties

3.1.1. Effect of Different Nano-Clay on Cracking of Cement Mortar

Based on the total crack length and total crack area of ordinary cement mortar specimens (A0), the total crack length ratio L and total crack area ratio M of each group of specimens were obtained. The maximum crack width, total crack length ratio L, total crack area ratio M, and crack reduction coefficient n of each group of specimens change with age is shown in Figure 3.

From Figure 3, it can be seen that the maximum crack width of specimen NMK-3 is 74.1%, 41.7%, and 46.7%, 33.3% lower than that of NMK-1, and NMA-2 crack reduction coefficient n of NMK-3 specimen is 150.0%, 38.9%, and 83.7%, 54.9% higher than that of NMK-1 and NMA-2, respectively. The crack reduction coefficient n of specimen NMK is 19.0% higher than that of specimen NMA. Compared with ordinary cement mortar specimens, the maximum crack width, maximum crack length, unit cracking area, total length ratio, and total cracking area ratio of NCM specimens are significantly reduced, and the crack prevention effect of the NMK specimens is more significant than that of the NMA specimens, indicating that the addition of nano-clay can inhibit the generation and development of cracks, compensating for the cracks and pores generated during cement hydration, and significantly improves the crack resistance of cement mortar. Under the same water–binder ratio, NMA greatly increases the viscosity of cement mortar compared with NMK, restrains the flow of water in suspension, and is not easy to evenly distribute in cement-based materials, resulting in a significant uneven distribution of hydration products. The overlap between the gels is not close enough to form a dense network structure, so the NMK specimen has better crack resistance than the NMA specimen.

3.1.2. Effect of Nano-Clayon Mechanical Properties of Cement Mortar

The mechanical properties of cement mortar with nano-clay under various curing agesareshown in Table 5.

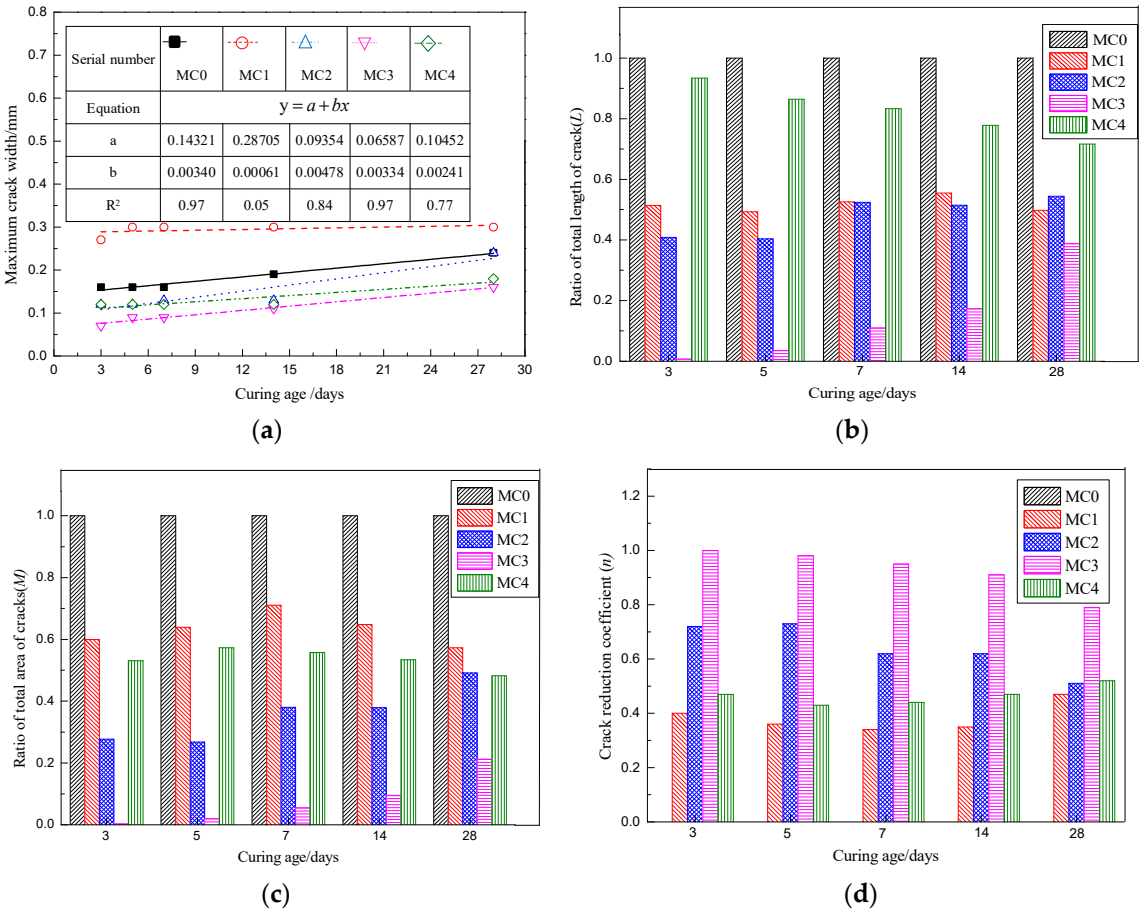


Figure 3. Maximum crack width, *L*, *M*, *n*, and age: (**a**) maximum crack width; (**b**) total crack length ratio *L*; (**c**) total cracking area ratio *M*; (**d**) crack reduction coefficient *n*.

Table 5. Mechanical properties under various curing ages.

Specimen Number	Category	Curing Age/Day				
		3	**7**	**14**	**28**	**60**
MC0	Flexural strength/MPa	4.4	5.0	6.0	7.1	7.5
MC1		3.9	5.5	6.1	7.2	7.7
MC2		3.5	4.4	5.3	6.1	6.7
MC3		4.6	5.6	6.6	7.3	8.4
MC4		4.0	4.9	5.8	6.7	7.2
MC0	Compressive strength/MPa	16.2	21.1	24.5	29.1	34.4
MC1		14.7	20.6	25.3	31.3	35.9
MC2		11.9	14.9	16.7	26.6	30.8
MC3		15.8	21.9	25.9	32.5	36.7
MC4		16.4	20.8	24.7	31.6	34.9
MC0	Tensile strength/MPa	0.99	1.45	1.77	2.07	2.38
MC1		1.04	1.52	1.86	2.18	2.5
MC2		0.93	1.36	1.67	1.95	2.24
MC3		1.07	1.56	1.91	2.23	2.56
MC4		1.05	1.53	1.88	2.19	2.51

The addition of NMK improves the flexural strengthand compressive strengthof cement mortar. The improvement effect of NMA on the mechanical properties of cement mortar is not obvious or even reduced. Compared with ordinary cement mortar specimens, the flexural strength of NMK-1 specimens is increased by 10.0% and 12.0% (7 d), the compressive strength is increased by 3.3% (14 d) and 3.8% (7 d). Compared with ordinary

cement mortar specimens, the flexural strength of the NMK-3 specimens was increased by 2.7% and 12.0% (60 d), the compressive strength was increased by 3.8% and 6.7% (60 d). The flexural strength and compressive strength of the NMA specimens were lower than those of ordinary cement mortar specimens. The compressive strength of the NMA-2 specimens was increased by 1.2% (3 days) and 1.5% (60 days) compared with ordinary cement mortar specimens. The flexural strength of the NMK-3 specimens was 1.8%, 27.3%,14.3% (7 days) and 9.1%, 25.4%, 16.7% (60 days) higher than that of NMK-1, NMA-1, and NMA-2 specimens, respectively. The compressive strength of the NMK-3 specimens was 6.3%, 47.0%, 5.3% (7 days) and 2.2%, 19.2%, and 5.2% (60 days) higher than that of the NMK-1, NMA-1, and NMA-2 specimens, respectively.According to these results, NMK with smaller particle sizes and active mineralscan effectively fill the larger pores of the cement mortar matrix, promoting the hydration reaction process of the cement mortar, increasingthe hydration products, and causingthe cement mortar to form a dense and hardened slurry, thereby improving the mechanical properties of the cement mortar; theseresults are in good agreement with the results of Zhang and Kawashima [13,14].

3.2. Fractal Description of Cracks

To more intuitively reveal the development trend of mechanical properties of the materials after cracking, and to avoid structural damage caused by traditional detection methods. Based on fractal theory, this section describes the irregularity of cracks on the surface of NCM plate specimens [15–18], and the fractal dimension of cracks on the surface of specimens is used as a characteristic parameter to quantitatively describe the cracks of the specimens. Figure 4 shows the log$N$-log$(1/r)$ relationship curve of crack distribution at the age of 28 days, and Figure 5 shows the relationship between the fractal dimension D_f and the age of surface cracks in each group. D_f is calculated according to Formula (4):

$$D_f = \mathrm{logN}/\log(1/\mathrm{r}) \tag{4}$$

where D_f is thefractal dimension and r is a measuring scale with the dimension of length [23].

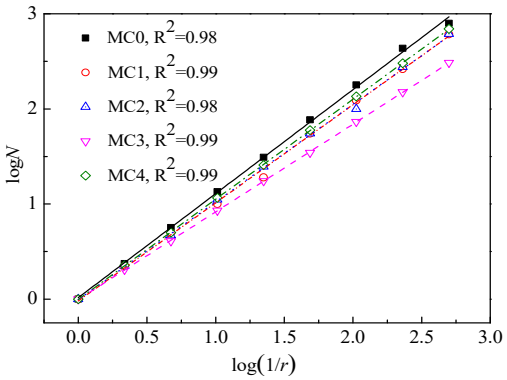


Figure 4. The log$N$-log$(1/r)$ curve under restrained conditions.

It can be seen from Figure 4 that there is a good linear relationship between log$N$ and log$(1/r)$ of propagating cracks inNCM specimens under the constraint of flat knife edge, and the surface crack distribution of NCM specimens has fractal characteristics.

From Figure 5, it can be seen that the fractal dimension of the surface cracksin the NCM specimen increases with the age of the power function. The growth rate of the fractal dimension of each group of specimens (except the A3 specimen) decreases with the increase in age, indicating that the cracking speed decreases. At 0–7 d, the growth rate of the fractal dimension of the surface cracksinthe NMA and NMK plates is smaller than that of the ordinary cement mortar specimen, indicating that the nano-clay makes the early cracking speed of the cement mortar decrease. Therefore, the slope of the fractal dimension D_f and the age curve can characterize the surface cracking degree of the cement mortar plate specimen; the fractal dimension of ordinary cement mortar is the largest (3 and 28 d), and

the fractal dimension of cracks on the surface of the NMK plate is smaller than that of the NMA specimen. In the same nano-clay, the smaller the particle size of the clay particles, the smaller the fractal dimension, and the smaller the crack area, length, and width. It shows that the fractal dimension reflects the cracking of the surface of the specimen and can be used as a quantitative evaluation index of cracks. The agglomerated particles of nano-clay effectively fill the pores in cement mortar and make the structure denser. The size of clay particles after dispersion determines the cracking on the surface of the plate specimen [22].

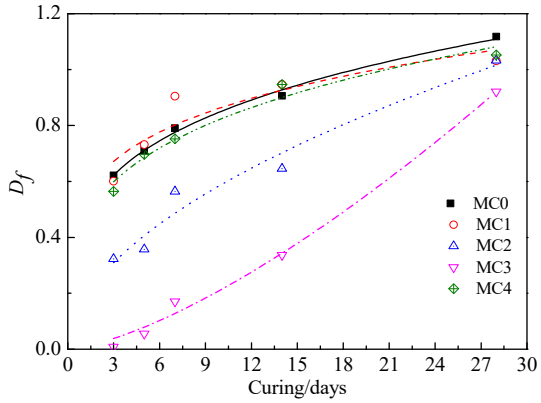


Figure 5. Relationship between fractal dimension and curing age.

3.3. Relationship between Fracture Fractal Dimension and Mechanical Properties of Nano-Clay Cement Mortar

3.3.1. Relationship between Fracture Fractal Dimension and Flexural Strength, Compressive Strength

NMK improves the mechanical properties of cement-based materials, but NMA, owing to its low activity, results in dispersed clay particle sizes that are too small, and the viscosity is too large, resulting in reduced mechanical properties of the cement-based materials. The environmental temperature difference has a great influence on the initial cracking time of the cement mortar. After adding NMK and NMA, the early hydration reaction is accelerated and the water demand becomes larger. Although the crack resistance of cement mortar is improved, the cracking time is earlier. The mechanical properties such as the elastic modulus, tensile strength, and compressive strength of NMK and NMA are important factors affecting the crack resistance, and the cracking situation can be characterized by fractal dimension. Therefore, this sectionproposes a prediction model forthe relationship between mechanical properties and fractal dimension through the relationship between fractal dimension and mechanical properties; this model reveals the influence of NCM mechanical properties on its crack resistance. The relationship between NCM flexural strengthand fractal dimension D_f, and the relationship between NCM 28 d fractal dimension $D_{f,28}$ and statistical parameters λ and φ are shown in Figure 6.

It can be seen from Figure 6 that the flexural strength of NCM increases with the fractal dimension D_f in a power function, and the statistical parameters λ and φ are linearly related to the 28 d fractal dimension $D_{f,28}$ of NCM. After adding nano-clay, the fractal dimension of NMK and NMA at each age is smaller than that of ordinary cement mortar, and its flexural strength is also larger, indicating that the flexural strength of nano-clay cement mortar with smaller fractal dimension is larger. With the increase infractal dimension D_f, the growth rate of flexural strength is basically unchanged (except for NMK-3). The growth rate of flexural strength forearly NMK is larger than that forordinary cement mortar specimens. The growth rate of flexural strength forordinary cement mortar specimens is larger than that forthe NMA specimens. The larger the particle size of clay agglomerates, the smaller the fractal dimension, indicating that the fractal dimension of NCM surface cracks can predict the flexural strength of different nano-clays and clays with different

particle sizes. The relationship between NCM flexural strength and fractal dimension D_f can be expressed as:

$$R_f(t) = \lambda D_f^{\varphi} \tag{5}$$

where $R_f(t)$ is the flexural strength of NCM at age t, MPa; t is the age, d; and λ and φ are statistical parameters.

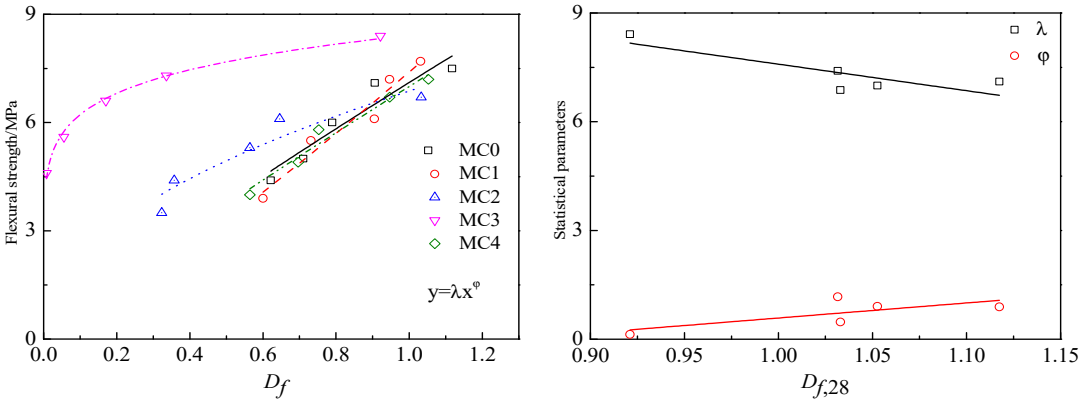


Figure 6. The relationship between flexural strength of NCM and statistical parameters and D_f: (**a**) R_f with D_f; (**b**) statistical parameters with $D_{f,28}$.

Through statistical analysis, the relationship between the 28 d fractal dimension $D_{f,28}$ of NCM and statistical parameters λ and φ can be expressed as:

$$\begin{cases} \lambda = -7.3D_{f,28} + 14.9 \\ \varphi = 4.2D_{f,28} - 3.6 \end{cases} \tag{6}$$

where λ and φ are statistical parameters.

Therefore, the prediction model forthe NCM flexural strength curve with fractal dimension D_f can be expressed as (4) and (5).

The relationship between NCM compressive strength and fractal dimension D_f and the relationship between NCM 28 d fractal dimension $D_{f,28}$ and statistical parameters λ and φ is shown in Figure 7.

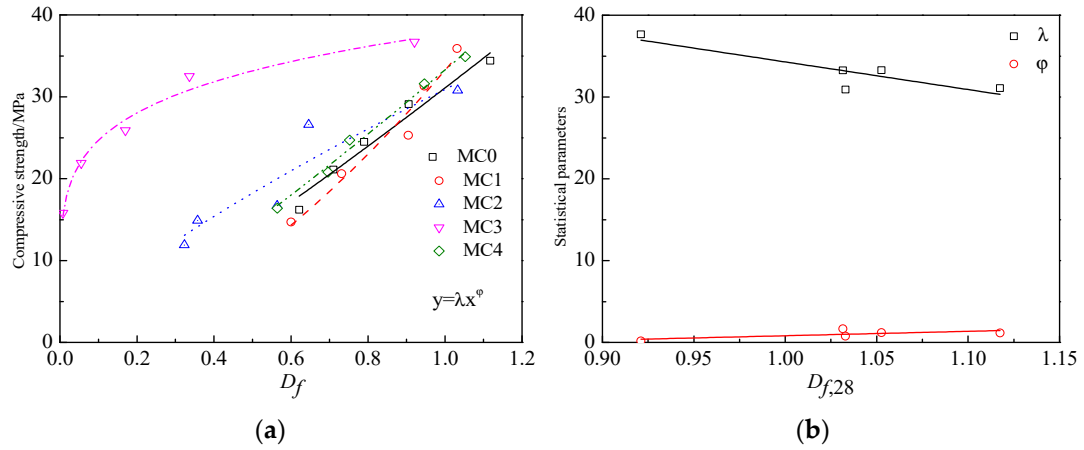


Figure 7. The relationship between compression strength of NCM and statistical parameters and D_f: (**a**) R_c with D_f; (**b**) statistical parameters with $D_{f,28}$.

It can be seen from Figure 7 that the compressive strength of NCM has anincreasing power function relationship with the fractal dimension D_f, and the statistical parameters λ

and φ have a linear correlation with the 28 d fractal dimension $D_{f,28}$ of NCM. The fractal dimension of NMK and NMA at each age is smaller than that forordinary cement mortar, and its compressive strength is also larger, indicating that the compressive strength of nano-clay cement mortar with a smaller fractal dimension is larger. With the increase infractal dimension D_f, the growth rate of compressive strength is unchanged (except NMK-3). The growth rate of compressive strength of early NMK is larger than that forordinary cement mortar specimens. The growth rate of compressive strength forordinary cement mortar specimens is larger than that for NMA specimens. The larger the particle size of clay agglomerates, the smaller the fractal dimension and the greater the compressive strength, indicating that the fractal dimension of NCM surface cracks can predict the compressive strength of different nano-clays and clays with different particle sizes. The relationship between NCM compressive strength and fractal dimension D_f can be expressed as:

$$R_c(t) = \lambda D_f^{\varphi} \tag{7}$$

where $R_c(t)$ is the flexural strength of NCM at t age, MPa; t is the age, d; and λ and φ are statistical parameters.

Through statistical analysis, the relationship between 28d fractal dimension $D_{f,28}$ of NCM and statistical parameters λ and φ can be expressed as:

$$\begin{cases} \lambda = -33.8D_{f,28} + 68.1 \\ \varphi = 5.4D_{f,28} - 4.6 \end{cases} \tag{8}$$

where λ and φ are statistical parameters.

Therefore, the prediction model forNCM flexural strength curve with fractal dimension can be expressed as (6) and (7).

3.3.2. Relationship between Fracture Fractal Dimension and Elastic Modulus

The relationship between NCM elastic modulus and age, fractal dimension D_f, and the relationship between NCM 28 d fractal dimension $D_{f,28}$ and statistical parameters λ and φ are shown in Figure 8.

From Figure 8, it can be seen that the elastic modulus of NCM increases exponentially with age, and power function with fractal dimension Df, respectively. The statistical parameters λ and φ are linearly correlated with the 28 d fractal dimension D_f, 28 of NCM. The fractal dimension of NMK and NMA at each age is smaller than that of ordinary cement mortar, and its elastic modulus is also larger, indicating that the elastic modulus of nano-clay cement mortar with smaller fractal dimension is larger. With the increase infractal dimension D_f, the growth rate of the elastic modulus increases gradually (except NMK-3). The growth rate of the elastic modulus of theNMK specimen is larger than that of the NMA specimen. The growth rate of the elastic modulus of theNMA specimen is larger than that of the ordinary cement mortar specimen. The larger the particle size of clay particles after dispersion, the smaller the fractal dimension is. The larger the early-age elastic modulus, the larger the growth rate is. The smaller the particle size of clay particles after dispersion leads to the decrease inthe elastic modulus, which indicates that the fractal dimension of NCM surface cracks can be used to infer the elastic modulus of different nano-clays and clays with different particle sizes.

The relationship between the elastic modulus *E(t)* and fractal dimension D_f of NCM can be expressed as:

$$E(t) = \lambda D_f^{\varphi} \tag{9}$$

In the formula, $E(t)$ is the elastic modulus of NCM at age t, MPa; t is the age, d; and λ and φ are statistical parameters.

Through statistical analysis, the relationship between 28 d fractal dimension $D_{f,28}$ of NCM and statistical parameters λ and φ can be expressed as:

$$\begin{cases} \lambda = -4.1D_{f,28} + 7.3 \\ \varphi = 7.8D_{f,28} - 6.7 \end{cases} \quad (10)$$

where λ and φ are statistical parameters.

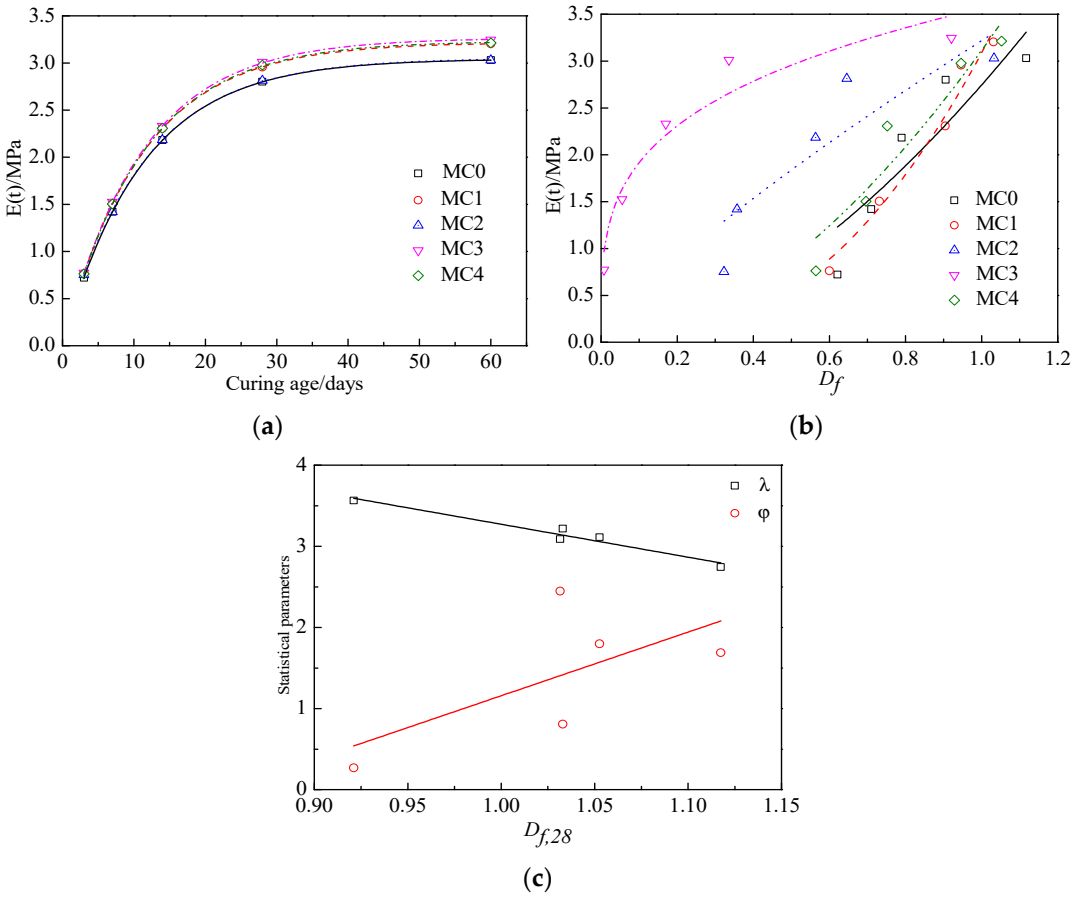


Figure 8. The relationship between modulus of elasticity and statistical parameters, curing age, and D_f: (**a**) $E(t)$ with age; (**b**) $E(t)$ with D_f; (**c**) statistical parameters with $D_{f,28}$.

Therefore, the prediction model for theNCM elastic modulus curve with fractal dimension can be expressed as (8) and (9).

The fractal dimension of NCM cracks not only intuitively reflects the law of crack development and quantitatively characterizes the degree of cracking, but also reveals the variation law of NCM strength during crack propagation, and establishes the relationship between NCM crack resistance and its strength. The strength can be directly judged by the fractal dimension. This method avoids the structural damage caused by core-sample drilling and the ultrasonic rebound synthesis method.

3.3.3. Relationship between Fracture Fractal Dimension and Tensile Strength

The relationship between NCM tensile strength and fractal dimension D_f is shown in Figure 9. From Figure 9, it can be seen that the tensile strength of NCM increases with the fractal dimension D_f in a power function, and the statistical parameters λ and φ are linearly correlated with the 28 d fractal dimension $D_{f,28}$ of NCM.

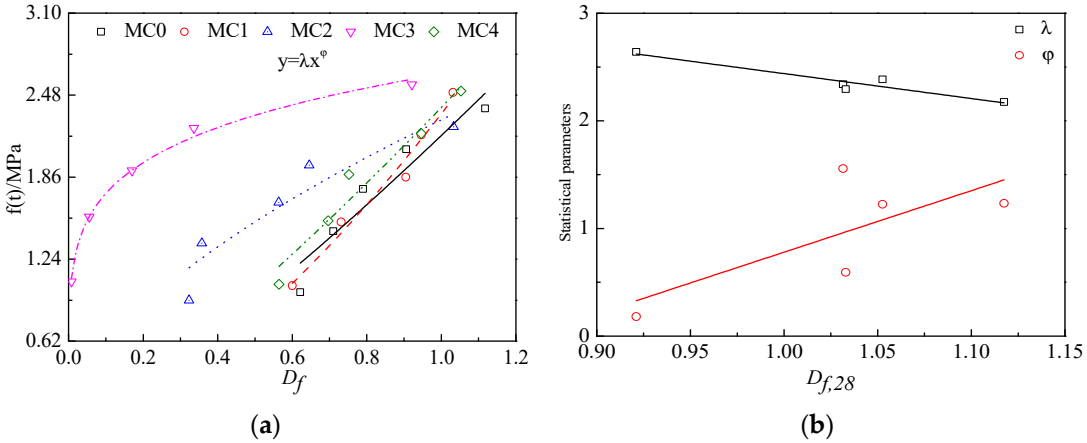


Figure 9. The relationship between tensile strength of NCM and statistical parameters and D_f: (**a**) $f(t)$ with D_f; (**b**) statistical parameters with $D_{f,28}$.

The fractal dimension of NMK and NMA at each age is smaller than that of ordinary cement mortar, and the tensile strength is also larger, indicating that the tensile strength of nano-clay cement mortar with a smaller fractal dimension is larger. With the increase infractal dimension D_f, the growth rate of tensile strength is unchanged (except NMK-3). The growth rate of tensile strength of the NMK specimens is larger than that of ordinary cement mortar specimens. The growth rate of tensile strength of ordinary cement mortar specimens is larger than that for theNMA specimens. The larger the particle size of clay particles after dispersion, the smaller the fractal dimension. The larger the tensile strength at an early age, the larger the growth rate is. The smaller the particle size of clay particles after dispersion, the lower the tensile strength is, indicating that the fractal dimension of NCM surface cracks can be used to infer the tensile strength of different nano-clays and clays with different particle sizes.

The relationship between NCM tensile strength *f(t)* and fractal dimension D_f can be expressed as:

$$f(t) = \lambda D_f^{\varphi} \tag{11}$$

where $f(t)$ is the tensile strength of NCM at t age, MPa; t is the age, d; and λ and φ are statistical parameters.

Through statistical analysis, the relationship between 28 d fractal dimension $D_{f,28}$ of NCM and statistical parameters λ and φ can be expressed as:

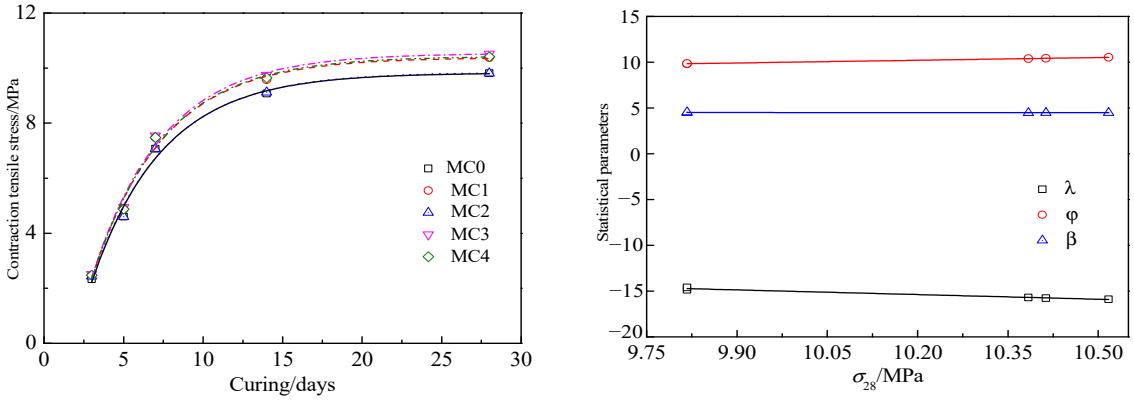
$$\begin{cases} \lambda = -2.3D_{f,28} + 4.8 \\ \varphi = 5.7D_{f,28} - 4.9 \end{cases} \tag{12}$$

where λ and φ are statistical parameters.

Therefore, the prediction model forthe NCM elastic modulus changing with fractal dimension D_f is expressed as (10) and (11).

3.3.4. Relationship between Fracture Fractal Dimension and Shrinkage Tensile Stress

The relationship between shrinkage tensile stress and the age of the NCM plate is shown in Figure 10. It can be seen from Figure 10 that the shrinkage tensile stress of the NCM plate increases exponentially with the age, and the statistical parameters λ, φ, and β are linearly related to the 28 d shrinkage tensile stress σ_{28} of NCM.



(**a**) (**b**)

Figure 10. The relationship between contraction tensile stressand statistical parameters and curing age: (**a**) $\sigma(t)$; (**b**) σ_{28}.

At 0-7d, the shrinkage tensile stress of NCM plate increases very fast. With the increase inage, the growth rate of shrinkage tensile stress decreases gradually. The growth rate of shrinkage tensile stress of NMK and NMA-2 specimens is larger than that forordinary cement mortar specimens. The growth rate of shrinkage tensile stress forordinary cement mortar specimens is basically the same as that of NMA-1. The larger the particle size of clay particles after dispersion, the larger the early age shrinkage tensile stress and the larger the growth rate. The smaller the particle size of clay particles after dispersion, the smaller the shrinkage tensile stress. It shows that NMK and NMA make the early shrinkage tensile stress of cement mortar plate larger and grow faster, and the particle size of clay particles after dispersion is larger. The shrinkage tensile stress is larger and the growth rate is also larger. The relationship between shrinkage tensile stress $\sigma(t)$ and age of NCM plate can be expressed as:

$$\sigma(t) = \lambda e^{-\frac{t}{\beta}} + \varphi \tag{13}$$

where $\sigma(t)$ is the shrinkage tensile stress of NCM at t age, MPa; t is the age, d; and λ, φ, and β are statistical parameters.

Through statistical analysis, the relationship between the shrinkage tensile stress σ_{28} of the NCM plate andthe statistical parameters λ, φ, and β can be expressed as:

$$\begin{cases} \lambda = -1.7\sigma_{28} + 1.9 \\ \varphi = \sigma_{28} + 0.1 \\ \beta = -0.03\sigma_{28} + 4.8 \end{cases} \tag{14}$$

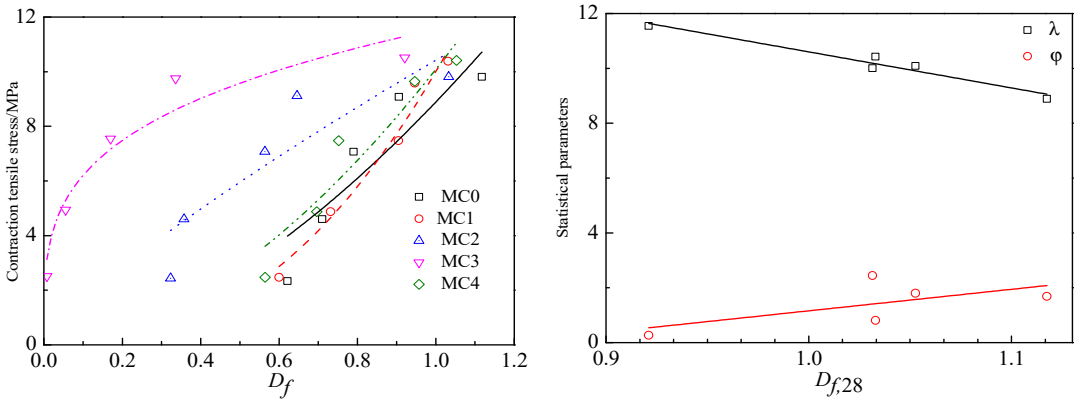
where σ_{28} is the shrinkage tensile stress of NCM at 28days, MPa; and λ, φ, and β are statistical parameters.

Therefore, the prediction model for the relationship between the shrinkage tensile stress of NCM plate and the age can be expressed by (12) and (13).

The relationship between NCM plate shrinkage tensile stress and fractal dimension D_f is shown in Figure 11. It can be seen from Figure 11 that the shrinkage tensile stress of NCM plate increases exponentially with the fractal dimension D_f, and the statistical parameters λ and φ are linearly correlated with the 28d fractal dimension $D_{f,28}$ of NCM.

The fractal dimension of NMK and NMA at each age is smaller than that forordinary cement mortar, and its shrinkage tensile stress is also larger, indicating that the shrinkage tensile stress of nano-clay cement mortar with smaller fractal dimension is larger. With the increase infractal dimension D_f, the growth rate of shrinkage tensile stress is basically unchanged(except NMK-3), and the growth rate of shrinkage tensile stress of the NMK and NMA-2 specimens is larger than that of ordinary cement mortar specimens. It shows that

the fractal dimension of NCM surface cracks can be used to predict the shrinkage tensile stress of different nano-clay and different particle size clay.



(**a**) (**b**)

Figure 11. The relationship between contraction tensile stress and statistical parameters and D_f: (**a**) $\sigma(t)$ with D_f; (**b**) statistical parameters with $D_{f,28}$.

The relationship between shrinkage tensile stress $\sigma(t)$ and fractal dimension D_f of NCM plate can be expressed as:

$$\sigma(t) = \lambda D_f^{\varphi} \tag{15}$$

where $\sigma(t)$ is the shrinkage tensile stress of NCM at t age, MPa; t is the age, d; and λ and φ are statistical parameters.

Through statistical analysis, the relationship between NCM plate shrinkage tensile stress $D_{f,28}$ and statistical parameters λ and φ can be expressed as:

$$\begin{cases} \lambda = -13.1D_{f,28} + 23.7 \\ \varphi = 7.8D_{f,28} - 6.7 \end{cases} \tag{16}$$

where λ and φ are statistical parameters.

Therefore, the prediction model forthe shrinkage tensile stress of NCM plate with the change infractal dimension D_f can be expressed as (14) and (15).

4. Conclusions

In this paper, the main conclusions are as follows:

(1) The cracking time of NMK-3 was 2 h and 6 h later than that forNMK-1 and NMA-2, respectively. After 28 days curing, the maximum crack width of specimen NMK-3 was 46.7% and 33.3% lower than that for NMK-1 and NMA-2 respectively. The crack reduction coefficient n of NMK specimen was 19.0% higher than that for specimen NMA.

(2) NMK with itssmaller particle size has the best improvement effect on cement mortar. The flexural strength ratioand compressive strength ratioat 7 d and 28 d are 76.7% and 67.4%, respectively. The improvement effect inNMK on the mechanical properties of cement mortar is due to NMA.

(3) The surface crack distribution in theNCM specimens has fractal characteristics;the larger the particle size of nano-clay, the smaller the fractal dimension.The larger the fracture area, length, and width, the larger the fractal dimension. Fracture fractal dimension can not only characterize the cracking degree of NCM, but also predict its elastic modulus and shrinkage tensile stress.

Author Contributions: Writing—original draft preparation, writing—review and editing, and funding acquisition, S.Z.; formal analysis, Z.F.; formal analysis, W.Q.; resources, formal analysis, and investigation, Y.F.; methodology, S.P.S. All authors have read and agreed to the published version of the manuscript.

Funding: This research was financially supported by the National NaturalScience Foundation of China (Grant No. 51908342), and by the NaturalScience Foundation of Shandong Province (Grant No. ZR2018PEE021, ZR2022ME133), to which the authors are very grateful.

Data Availability Statement: Not applicable.

Conflicts of Interest: The authors declare no conflict of interest.

References

1. El-Gamal, S.M.A.; Hashem, F.S.; Amin, M.S. Influence of carbon nanotubes, nanosilica and nanometakaolin on some morphological-mechanical properties of oil well cement pastes subjected to elevated water curing temperature and regular room air curing temperature. *Constr. Build. Mater.* **2017**, *146*, 531–546. [CrossRef]
2. Liu, G.; Zhang, S.; Fan, Y.; Shah, S.P. Study on Shrinkage Cracking Morphology of Cement Mortar with Different Nanoclay Particles under Restraint. *Buildings* **2022**, *12*, 1459. [CrossRef]
3. Rong, Z.; Zhao, M.; Wang, Y. Effects of Modified Nano-SiO_2 Particles on Properties of High-Performance Cement-Based Composites. *Materials* **2020**, *13*, 646. [CrossRef] [PubMed]
4. Zhang, P.; Han, Q.; Wu, J.; Zhang, Y.; Zhang, T. Mechanical properties of nano-SiO_2 reinforced engineered cementitious composites after exposure to high temperatures. *Constr. Build. Mater.* **2022**, *356*, 129123. [CrossRef]
5. Zhang, P.; Yuan, P.; Guan, J.; Guo, J. Fracture behavior of multi-scale nano-SiO_2 and polyvinyl alcohol fiber reinforced cementitious composites under the complex environments. *Theor. Appl. Fract. Mec.* **2022**, *122*, 103584. [CrossRef]
6. Han, Q.; Zhang, P.; Wu, J.; Jing, Y.; Zhang, D.; Zhang, T. Comprehensive review of the properties of fly ash-based geopolymer with additive of nano-SiO_2. *Nanotechnol. Rev.* **2022**, *11*, 1478–1498. [CrossRef]
7. Ren, J.; Zhang, L.; Zhao, H.; Zhao, Z.; Wang, S. Determination of the fatigue equation for the cement-stabilized cold recycled mixtures with road construction waste materials based on data-driven. *Int. J. Fatigue* **2022**, *158*, 106765. [CrossRef]
8. Xin, J.D.; Zhang, G.X.; Liu, Y.; Wang, Z.; Wu, Z. Effect of temperature history and restraint degree on cracking behavior of early-age concrete. *Constr. Build. Mater.* **2018**, *192*, 381–390. [CrossRef]
9. Cao, J.; Jin, Z.; Ding, Q.; Xiong, C.; Zhang, G. Influence of the dry/wet ratio on the chloride convection zone of concrete in a marine environment. *Constr. Build. Mater.* **2022**, *316*, 125794. [CrossRef]
10. Ren, J.; Zhao, H.; Zhang, L.; Zhao, Z.; Xu, Y.; Cheng, Y.; Wang, M.; Chen, J.; Wang, J. Design optimization of cement grouting material based on adaptive boosting algorithm and simplicial homology global optimization. *J. Build. Eng.* **2022**, *49*, 104049. [CrossRef]
11. Douba, A.E.; Ma, S.; Kawashima, S. Rheology of fresh cement pastes modified with nanoclay-coated cements. *Cem.Concr. Comp.* **2022**, *125*, 104301. [CrossRef]
12. Zhang, S.; Fan, Y.; Shah, S.P. Study on Deformation Characteristics and Damage Model of NMKConcrete under Cold Environment. *Buildings* **2022**, *12*, 1431. [CrossRef]
13. Zhang, S.; Fan, Y.; Huang, J.; Shah, S.P. Effect of nano-metakaolinite clay on the performance of cement-based materials at early curing age. *Constr. Build. Mater.* **2021**, *291*, 123107. [CrossRef]
14. Kawashima, S.; Wang, K.; Ferron, R.D.; Kim, J.H.; Shah, S. A review of the effect of nanoclays on the fresh and hardened properties of cement-based materials. *Cem. Concr. Res.* **2021**, *147*, 106502. [CrossRef]
15. Wilkie, S.; Dyer, T. Design and durability of early 20Th century concrete bridges in Scotland: A review of historic test data. *Int. J. Arch. Herit.* **2022**, *16*, 1131–1151. [CrossRef]
16. Ren, J.; Xu, Y.; Zhao, Z.; Chen, J.; Cheng, Y.; Huang, J.; Yang, C.; Wang, J. Fatigue prediction of semi-flexible composite mixture based on damage evolution. *Constr. Build. Mater.* **2022**, *318*, 126004. [CrossRef]
17. Liu, P.; Chen, Y.; Sha, F.; Yu, Z.; Shao, G. Study on micro structure and composition distribution of concrete surface zone based on fractal theory and XCT technology. *Constr. Build. Mater.* **2020**, *263*, 120209. [CrossRef]
18. Rezaie, A.; Mauron, A.J.; Beyer, K. Sensitivity analysis of fractal dimensions of crack maps on concrete and masonry walls. *Automat. Constr.* **2020**, *117*, 103258. [CrossRef]
19. Zheng, D.; Song, W.D.; Fu, J.X.; Xue, G.; Li, J.; Cao, S. Research on mechanical characteristics, fractal dimension and internal structure of fiber reinforced concrete under uniaxial compression. *Constr. Build. Mater.* **2020**, *258*, 120351. [CrossRef]
20. Zhu, D.Q.; Tang, A.P.; Wan, C.L.; Zeng, Y.; Wang, Z. Investigation on the flexural toughness evaluation method and surface cracks fractal characteristics of polypropylene fiber reinforced cement-based composites. *J. Build. Eng.* **2021**, *43*, 103045. [CrossRef]
21. Szeląg, M. Fractal characterization of thermal cracking patterns and fracture zone in low-alkali cement matrix modified with microsilica. *Cem. Concr. Compos.* **2020**, *114*, 103732. [CrossRef]
22. Guo, Z.P.; Liu, W.Z.; Wang, C.; He, C.; Zhang, F. Fractal characteristics of mesostructure and optimization of axial compression constitutive model of coal-fired slag concrete. *Mater. Today Commun.* **2021**, *28*, 102686. [CrossRef]

23. Zamen, S.; Dehghan-Niri, E. Fractal analysis of nonlinear ultrasonic waves in phase-space domain as a quantitative method for damage assessment of concrete structures. *NDT E Int.* **2020**, *111*, 102235. [CrossRef]
24. Zhou, M.; Xu, L.Y.; Tao, M.X.; Fan, J.S.; Hajjar, J.F.; Nie, J.G. Experimental study on confining-strengthening, confining-stiffening, and fractal cracking of circular concrete filled steel tubes under axial tension. *Eng. Struct.* **2017**, *133*, 186–199. [CrossRef]
25. Mei, Y.; Zhang, A.; Shen, J.; Wu, B.; Wei, X. A fractal comminution approach for scaling issues of penetration failure of concrete target. *Eng. Fail. Anal.* **2022**, *140*, 106553. [CrossRef]
26. Liu, Y.; Dai, K.; Li, D.; Luo, M.; Liu, Y.; Shi, Y.; Xu, J.; Huang, Z. Structural performance assessment of concrete components based on fractal information of cracks. *J. Build. Eng.* **2021**, *43*, 103177. [CrossRef]
27. Zhang, P.; Gao, Z.; Shi, Y.; Lin, Y.; Li, J. Effect of large broken stone content on properties of roller compacted concrete based on fractal theory. *Constr. Build. Mater.* **2020**, *262*, 120821. [CrossRef]

Disclaimer/Publisher's Note: The statements, opinions and data contained in all publications are solely those of the individual author(s) and contributor(s) and not of MDPI and/or the editor(s). MDPI and/or the editor(s) disclaim responsibility for any injury to people or property resulting from any ideas, methods, instructions or products referred to in the content.